Geometry of Optimal Control in Chemical Reaction Networks in the Adiabatic Limit

Yikuan Zhang,[1] Qi Ouyang,[2,3] and Yuhai Tu[4]
[1]School of Physics, Peking University, Beijing 100871, China
[2]Institute for Advanced Study in Physics, Zhejiang University, Hangzhou 310058, China
[3]Center for Quantitative Biology, AAIC, Peking University, Beijing 100871, China
[4]IBM T. J. Watson Research Center, Yorktown Heights, New York 10598, USA

(Received 7 July 2024; accepted 27 November 2024; published 6 January 2025)

Although optimal control (OC) has been studied in stochastic thermodynamics for systems with continuous state variables, less is known in systems with discrete state variables, such as chemical reaction networks (CRNs). Here, we develop a general theoretical framework to study OC of CRNs for changing the system from an initial distribution of states to a final distribution with minimum dissipation. We derive a "Kirchhoff's law" for the probability current in the adiabatic limit, from which the optimal kinetic rates are determined analytically for any given probability trajectory allowed by local rate constraints. By using the optimal rates, we show that the total dissipation is determined by a L_2-distance measure in the probability space and derive an analytical expression for the metric tensor that depends on the probability distribution, network topology, and capacity of each link. Minimizing the total dissipation leads to the geodesic trajectory in the probability space and the corresponding OC protocol is determined by the Kirchhoff's law. To demonstrate our general approach, we use it to find a lower bound for the minimum dissipation that is tighter than existing bounds obtained with only global constraints in the adiabatic limit. We also apply it to simple networks, e.g., fully connected three-state CRNs with different local constraints and show that indirect pathway and nonfunctional transient state can play a crucial role in switching between different probability distributions efficiently. Future directions in studying OC in CRNs by using our general framework are discussed.

DOI: 10.1103/PhysRevLett.134.018001

Most biological systems operate out of thermal equilibrium by constantly dissipating energy and exchanging matter and information with their environment. Despite their high noise level, biological systems can control (regulate) the underlying biochemical networks to achieve different biological functions accurately driven by chemical energy dissipation from hydrolysis of high energy molecules such as ATP and GTP [1–14]. As control theory gains attention in biology in recent years [15–18], an important general problem is to identify the optimal control process (protocol) to achieve certain biological function with minimal energy dissipation, i.e., the optimal control (OC) problem.

Within the fields of finite-time thermodynamics and stochastic thermodynamics, much work has been done in finding the optimal protocol that leads to the minimum total entropy production during thermodynamic processes [19–38], especially in systems with continuous state variables that can be described by overdamped Langevin dynamics [19–21,26–31].

However, for systems with discrete state variables such as chemical reaction networks (CRNs), most of the existing work focused on establishing lower bounds of the total entropy production [39–44] without considering OC. For example, Vu *et al.* computed dissipation in systems with given time-dependent transition rates that satisfy instantaneous detailed balance condition, yielding a lower bound without considering the OC problem [40]. By using the Wasserstein distance on graphs, Dechant obtained a lower bound with the global constraint of fixed total reaction activity [42]. Muratore-Ginanneschi *et al.*, did consider the OC problem but only for a continuous-time Markov jump process in one-dimensional countable state space [45].

Given that most biological systems are governed by biochemical networks with discrete state variables, we aim to develop a general theoretical framework to study the OC problem in CRNs under realistic constraints here.

The OC problem in discrete systems—In a CRN with N states, the transitions among these states are described by the chemical master equation

$$\frac{dP_i}{dt} = \sum_j (k_{ji}P_j - k_{ij}P_i), \quad i = 1, 2, 3, \ldots, N, \quad (1)$$

where $P_i(t)$ is the probability in state i at time t and k_{ij} is the transition probability rate from state i to state j.

The goal of the control process is to change the probability distribution of the system from $\mathbf{P}(0)$ to a final distribution $\mathbf{P}(\tau)$ by changing the $(N \times N)$ transition rate matrix $\mathbf{K}(t)$ during $0 \le t \le \tau$. During this control process,

the total energy dissipation is given by the total entropy production ($k_BT = 1$)

$$\mathcal{C}[\mathbf{K}(t)] = \int_0^\tau \dot{S}[\mathbf{K}(t), \mathbf{P}(t)]dt, \tag{2}$$

where $\dot{S}(t) = \frac{1}{2}\sum_{ij}(k_{ij}P_i - k_{ji}P_j)\ln(k_{ij}P_i/k_{ji}P_j)$ is the dissipation rate at time t [46].

The optimal control problem is to find the optimal protocol $\mathbf{K}(t)$ that minimizes the cost $\mathcal{C}[\mathbf{K}(t)]$ for changing the probability distribution from an initial probability distribution $\mathbf{P}(0)$ for $t \le 0$ to the final distribution $\mathbf{P}(\tau)$ for $t \ge \tau$. Following previous work [19,24], we allow rates to have discontinuous jumps at $t = 0$ and $t = \tau$.

Since each bidirectional reaction has different reactants and can be controlled by different enzymes, its reaction rates (k_{ij} and k_{ji}) are subject to reaction-specific constraint. For simplicity, we impose a reaction-specific constraint: $k_{ij} + k_{ji} = C_{ij}$ with C_{ij} a constant local rate capacity for link ij. Other local constraints can be used without affecting the general results (see the three-state gene circuit example for another choice of local constraints). An alternative is to constrain the time-averaged global reaction activities $\bar{A} \coloneqq (1/\tau)\int_0^\tau dtA(t), A = \sum_{i>j} P_i k_{ij}$ [39,42,43], which is less realistic given that individual reactions may be subject to different constraints.

The two-step optimization scheme—In general, OC is a difficult problem involving solving a nonlocal Euler-Lagrange equation numerically in the joint rate-probability space [19,25,45]. Here, we adopt a two-step optimization scheme to make the problem more tractable analytically, which leads to deeper insights about the OC protocol beyond numerical solutions.

The first step is to find the optimal $\mathbf{K}^*(t)$ for any given probability trajectory $\mathbf{P}(t)$ allowed by the local constraints, similar to the approach used by Ilker *et al.* [18]. For a given $\mathbf{P}(t)$, the chemical master equation [Eq. (1)] can be considered as a set of linear equations for $\mathbf{K}(t)$. Since the number of control variables (i.e., the number of k_{ij}) is larger than N, there are many solutions for $\mathbf{K}(t)$, and the first step of optimization is to find the optimal rates $\mathbf{K}^*[\mathbf{P}(t), \dot{\mathbf{P}}(t)]$ that minimizes the entropy production $\mathcal{C}[\mathbf{K}(t)]$.

The second step of optimization is then to find the optimal $\mathbf{P}^*(t)$ trajectory for given initial and final distributions $\mathbf{P}(0)$, $\mathbf{P}(\tau)$ to minimize the entropy production:

$$\mathbf{P}^*(t) = \arg\min_{\mathbf{P}} \int_0^\tau \dot{S}\{\mathbf{K}^*[\mathbf{P}(t), \dot{\mathbf{P}}(t)], \mathbf{P}(t)\}dt, \tag{3}$$

which reduces to a variational problem with regard to $\mathbf{P}(t)$. Solving the resulting Euler-Lagrange equation for $\mathbf{P}(t)$ leads to the optimal probability trajectory $\mathbf{P}^*(t)$.

Analogy to electronic circuit—For the rest of the Letter, we will work in the adiabatic limit when the relaxation time of the system τ_R is much shorter than τ. In this limit, we have $|1 - P_i k_{ij}/P_j k_{ji}| = \mathcal{O}(\tau_R/\tau) \ll 1$, and the total dissipation $\mathcal{C}(\mathbf{K})$ can be approximated as

$$\mathcal{C}_a(\mathbf{K}) = \int_0^\tau \sum_{ij} \frac{(P_i k_{ij} - P_j k_{ji})^2}{P_i k_{ij} + P_j k_{ji}} dt = \int_0^\tau \sum_{ij} J_{ij}^2 R_{ij} dt, \tag{4}$$

which is analogous to the Joule's law for electronic circuit. Here, the subscript "a" refers to the adiabatic limit. As shown in Fig. 1(b), $J_{ij} = -J_{ji} = P_i k_{ij} - P_j k_{ji}$ is the net current from node i to node j; $R_{ij} = R_{ji} = (P_i k_{ij} + P_j k_{ji})^{-1} \approx (1/2C_{ij})[(1/P_i(t)) + (1/P_j(t))]$ is the resistance for link ij [47]; P_i is the charge at node i. Since P_i depends on time (for changing probability), there is an input (driving) current source $J_i(t) = -\dot{P}_i(t)$ at each node-i with the constraint $\sum_i J_i = 0$ due to charge conservation.

From the circuit analogy, the first step in solving the OC problem becomes optimizing $\mathcal{C}_a$ in Eq. (4) with the current conservation constraint $J_i(t) = \Sigma_j J_{ij}(t)$ at each node i. By introducing a Lagrange multiplier $V_i(t)$ analogous to the voltage at node i, we can solve this optimization problem in the functional space of J_{ij} to obtain

$$\sum_j J_{ij} = \sum_j (V_i - V_j)/R_{ij} = J_i(t) = -\dot{P}_i(t), \quad \forall\ i, \tag{5}$$

which is the Kirchhoff's law for the CRN circuit.

By introducing the conductance matrix $\mathbf{\Gamma}(\mathbf{R})$ with $\Gamma_{ii} = -\sum_j R_{ij}^{-1}$ and $\Gamma_{ij} = R_{ij}^{-1}$ $(i \ne j)$, Eq. (5) can be solved (formally): $\mathbf{V} = \mathbf{\Omega}\dot{\mathbf{P}}$ with $\mathbf{\Omega} \equiv \mathbf{\Gamma}^{-1}$ [48]. The optimal current for a given $\mathbf{P}(t)$ can then be obtained: $J_{ij} = \sum_k (\Omega_{ik} - \Omega_{jk})R_{ij}^{-1}\dot{P}_k \equiv \sum_k \Phi_{ij,k}(\mathbf{R})\dot{P}_k$, where $\Phi_{ij,k}(\mathbf{R}) = (\Omega_{ik} - \Omega_{jk})R_{ij}^{-1}$ is a $(L \times N)$ matrix with L the number of transitions in the network.

The dissipation metric and geodesic trajectory in probability space—By using the optimal control protocol for given probability trajectory $\mathbf{P}(t)$, we obtain an analytical expression for the total dissipation rate in the probability space with a quadratic form in $\dot{\mathbf{P}}$,

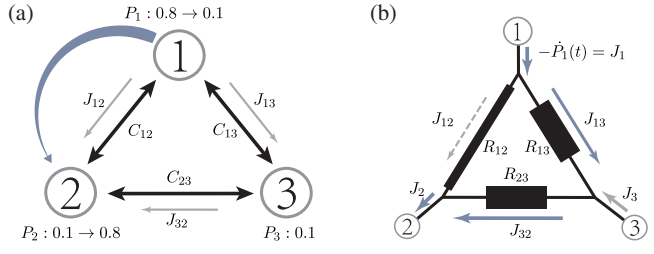

FIG. 1. The circuit analogy of CRN. (a) The optimal control problem of the smallest CRN, a fully connected thee-state network. (b) The corresponding electronic circuit.

$$\dot{S}_a(\mathbf{P}) = \sum_{ij} \Lambda_{ij}(\mathbf{R}) \dot{P}_i \dot{P}_j, \tag{6}$$

where $\Lambda_{ij}(\mathbf{R}) \equiv \Sigma_{kl} \Phi(\mathbf{R})_{kl,i} \Phi(\mathbf{R})_{kl,j} R_{kl}$ is defined as the "dissipation metric," which depends on $\mathbf{P}$ and the capacity matrix $\mathbf{C}$ through its direct dependence on $\mathbf{R}$. A similar expression for $\dot{S}_a(\mathbf{P})$ was obtained by Ilker *et al.* [18].

The dissipation rate given by Eq. (6) transforms the original OC problem defined in the $\mathbb{R}_+^L$ rate space to an optimal transport problem in the smaller $\mathbb{R}_+^{N-1}$ probability space. Minimizing the total dissipation $\mathcal{C}_a = \int_0^\tau \dot{S}_a dt$ with respect to $\mathbf{P}$ leads to the geodesic equation governing the dynamics of the optimal probability trajectory $\mathbf{P}^*$ [49],

$$\ddot{P}_i^* + \sum_{j,k=1}^{N-1} \mathcal{K}_{jk}^i \dot{P}_j^* \dot{P}_k^* = 0, \tag{7}$$

where $\mathcal{K}_{jk}^i \equiv \frac{1}{2} \sum_l (\Lambda^{*-1})_{li} (\partial_{P_k} \Lambda_{lj}^* + \partial_{P_j} \Lambda_{lk}^* - \partial_{P_l} \Lambda_{jk}^*)$ are Christoffel symbols with $\mathbf{\Lambda}^*$ the reduced dissipation metric by taking into account the constraint $\sum_i^N P_i = 1$ [see Sec. I in Supplemental Material (SM) [58] for details].

Solving the geodesic equation [Eq. (7)] with the "boundary" probabilities at $t = 0$ and $t = \tau$, we obtain the optimal probability trajectory $\mathbf{P}^*(t)$, which leads to an exact expression for the minimum dissipation $\mathcal{C}_{a,m}$,

$$\mathcal{C}_{a,m} \equiv \min(\mathcal{C}_a) = \int_0^\tau \sum_{i,j=1}^{N-1} \Lambda_{ij}^*(\mathbf{R}) \dot{P}_i^* \dot{P}_j^* dt. \tag{8}$$

More importantly, by using the Kirchhoff's Law, we obtain the corresponding OC protocol, $k_{ij}^* = (P_i^* + P_j^*)^{-1} (P_j^* C_{ij} + \sum_k \Phi_{ij,k} \dot{P}_k^*)$ (see Sec. I in SM for details).

The dissipation metric can be used to define a "dissipation length" in the probability space: $\mathcal{L}(\mathbf{P}) \equiv \int_0^\tau \sqrt{\sum_{i,j=1}^{N-1} \Lambda_{ij}^*(\mathbf{R}) \dot{P}_i \dot{P}_j} dt$. It is clear that the dissipation length is minimum at the optimal probability trajectory $\mathcal{L}_m \equiv \min(\mathcal{L}) = \mathcal{L}(\mathbf{P}^*)$, which is related to the minimum dissipation $(\mathcal{C}_{a,m})$ by $\mathcal{L}_m = \sqrt{\tau \mathcal{C}_{a,m}}$; see Sec. I.B in SM for details.

The Kirchhoff bound—Our approach can be used to establish a lower bound for the total entropy production in the adiabatic limit. In this limit, we have $R_{ij} \approx (1/2C_{ij})[(1/P_i(t)) + (1/P_j(t))] \geq 2/(C_{ij}(P_i + P_j)) > 2/C_{ij}$, which leads to the inequality $\mathcal{C}_a > \tilde{\mathcal{C}}_a \equiv \int_0^\tau 2 \sum_{ij} (J_{ij}^2 / C_{ij}) dt$, where $\tilde{\mathcal{C}}_a$ is the total dissipation for a simple system where the resistance for link ij is a constant $(2/C_{ij})$. For such a simple system, the metric matrix $\mathbf{\Lambda}$ becomes independent of $\mathbf{P}$, which corresponds to a flat manifold with $\mathcal{K}_{jk}^i = 0$ in the geodesic equation. Solving Eq. (7) leads to a linear optimal probability trajectory $P_i^*(t) = P_i(0) + \Delta P_i(t/\tau)$, where $\Delta P_i = P_i(\tau) - P_i(0)$, from which the minimum dissipation $\mathcal{C}_{a,kh} \equiv \min(\tilde{\mathcal{C}}_a)$ can be determined. It is clear that $\mathcal{C}_{a,kh}$, which is called the Kirchhoff bound, sets a lower bound for the total dissipation of the original system,

$$\mathcal{C}_a > \tilde{\mathcal{C}}_a \geq \mathcal{C}_{a,kh} = \Delta \mathbf{P}^T \mathbf{R}^* \Delta \mathbf{P} / \tau, \tag{9}$$

where R_{ij}^* is the effective resistance that contains the topological information of the CRN and strengths of its links (C_{ij}) (see Sec. II.A in SM for the expression of R_{ij}^* and the detailed proof of the Kirchhoff's bound).

The Kirchhoff bound [Eq. (9)] is generally applicable to any CRN. To understand its physical meaning, we computed the Kirchhoff bound explicitly for the transport process of a fully connected three-state network [Fig. 1(a)],

$$\mathcal{C}_{a,kh} = 2 \frac{\|\mathbf{P}(0) - \mathbf{P}(\tau)\|^2}{[C_{12} + C_{13} C_{23} / (C_{13} + C_{23})] \tau}, \tag{10}$$

which has an intuitive interpretation: the numerator quantifies the amount of probability that needs to be transported, and the denominator is the effective conductance of the network.

We have compared the Kirchhoff bound with existing lower bounds [42,43] obtained based on Wasserstein distance on graph $\mathcal{W}_1(p(0), p(\tau))$ with a global constraint by getting rid of the $P(t)$ dependence of this constraint using the same inequality to $R_{ij}(t)$. We found that the Kirchhoff bound $\mathcal{C}_{a,kh}$ is closer to the exact numerical value of the minimum entropy production than the Wasserstein bound $\mathcal{C}_{a,wst}$ (see Sec. II in SM for details). Intuitively, $\mathcal{C}_{a,wst}$ results from connecting all the channels 1-2, 1-3, and 3-2 in parallel regardless of the structure of the network, whereas $\mathcal{C}_{a,kh}$ is derived from the Kirchhoff's law that contains the topological information of the CRN, which makes $\mathcal{C}_{a,kh}$ a tighter bound.

Modes of optimal probability transport—Next, we applied our approach to study the OC problem in simple networks such as the two-state model, which can be solved analytically; see Sec. I.C in SM for details. Here, we study the optimal control of changing the distribution from predominately in state-1 (P1 = 0.8, P2 = P3 = 0.1) at t = 0 to predominantly in state-2 (P2 = 0.8, P1 = P3 = 0.1) in the fully connected three-state model [Fig. 1(a)].

There are two paths to move from state-1 to state-2: a direct path $1 \to 2$, and an indirect path $1 \to 3 \to 2$. For simplicity, we fixed the capacity of the direct path $C_{12} = 5$ and studied the optimal transport processes for different C_{23} and C_{13}. In Fig. 2(a), the percentage of direct transport $(1 \to 2)$ is shown in the space of relative capacities $(C_{13}/C_{12}, C_{23}/C_{12})$. In the lower left corner (black area) where $C_{12} \gg \min(C_{13}, C_{23})$, most of the probability transport goes through the direct path 1-2; whereas in the upper right corner (red area), where $C_{12} \ll \min(C_{13}, C_{23})$, most

of the probability flows through the indirect path 1-3-2. Interestingly the critical line (red line), where the percentage is 50%, is close to the line $C_{12} = C_{13}C_{23}/(C_{13} + C_{23})$, where the effective resistance of the direct and indirect paths are equal.

To understand the modes of optimal probability transport, we studied the geodesics in probability space for different choices of the parameters $(C_{13}/C_{12}, C_{23}/C_{12})$. In Figs. 2(b) and 2(c), two typical geodesics are shown in the probability space for the direct and indirect dominated transport regimes, respectively. Generally, the geodesics go through the region where the metric is small to minimize the dissipation length. For the case of direct path dominated transport shown in Fig. 2(b), the metric is smaller near the diagonal $(P_1 + P_2 = 1)$, where $P_3 = 1 - (P_1 + P_2) = 0$, which attracts the geodesic there leading to a direct path with small P_3. But for the indirect transport case shown in Fig. 2(c), the region of small metric is away from the diagonal, leading to the indirect geodesic path that goes through a region with high P_3. See Secs. I.C and III.A in SM for details of the geodesics in other parts of the parameter space and the full OC "Phase-Diagram."

A three-state gene circuit—Finally, to show how the $P_i(t)$-dependent $R_{ij}(t)$ affects the optimal protocols in a realistic system, we studied a gene switching model [18]. As shown in Fig. 3(a), the gene has three states: state-1 is the open state that can bind with RNA polymerase to transcribe, state-2 is the partially closed state binding a bare repressor protein, and state-3 is the fully closed state binding a repressor-corepressor complex, which has a much lower dissociation constant compared with that of state-2 ($k_{-x} = 0.072\ \text{min}^{-1} \ll k_{-r} = 1.68\ \text{min}^{-1}$).

We consider the switching process from the open state-1 $(P_1 = 0.9,\ P_2 = 0.05,\ P_3 = 0.05)$ to the fully closed state-3 $(P_1 = 0.05,\ P_2 = 0.05,\ P_3 = 0.9)$ within a time window $\tau(= 5[\text{min}])$ after receiving some upstream signals. The transitions between different gene states are mediated by binding or unbinding reactions. Here, instead of fixing the total reaction rates $\{C_{ij}\}$ for each binding or unbinding reaction, the dissociation rates (k_{-r}, k_{-c}, k_{-x}) are fixed. The goal of OC is to control the binding rates by controlling the concentrations $R(t)$ (bare repressor), $C(t)$ (corepressor), and $X(t)$ (repressor-corepressor complex) in order to switch the gene state with minimum dissipation.

By using the circuit analogy, we find that the resistances for each reaction are $R_{12}(t) = (1/2k_{-r})(1/P_2(t))$, $R_{23}(t) = (1/2k_{-c})(1/P_3(t))$, $R_{13}(t) = (1/2k_{-x})(1/P_3(t))$ for a given $\mathbf{P}(t)$. By solving the OC problem with the two-step scheme, we obtained the optimal protocol and probability trajectory shown in Figs. 3(b)–3(c) (see Fig. S11 in SM for details). The lower dissociation constant in reaction path 1-3 causes a larger cost for direct transition from state-1 to state-3. Thus, the optimal protocol is to drive most of probability flow through indirect pathway $1 - 2 - 3$ rather than the direct pathway 1-3. Although state-2 is not the target state, P_2 accumulates transiently as it serves as a buffer to minimize the total dissipation. If we remove state-2, the probability has to transport from state-1 to state-3 directly, and the energy cost for this two-state model is higher than the three-state model as shown in Fig. 3(d). However, the difference diminishes as k_{-x} increases when the direct path 1-3 becomes the energetically preferred switching path.

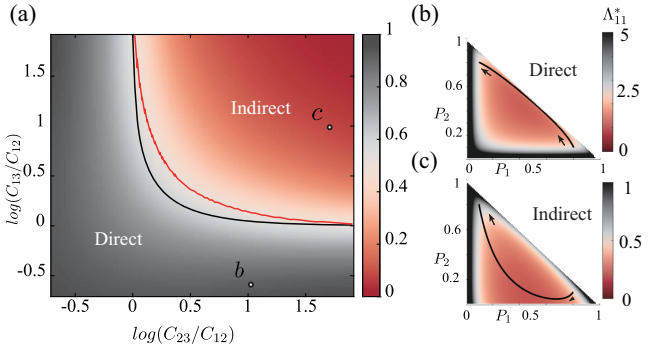

FIG. 2. (a) Phase diagram shown for given $C_{12} = 5$ and $\tau = 5$. The color represents the percentage of transport by the direct link 1-2 versus the indirect route 1-3-2. The black line is the line where $C_{12} = C_{13}C_{23}/(C_{13} + C_{23})$. The red line is the exact critical line where the percentage is 1/2. (b),(c) The reduced metric element $\Lambda^*_{11}(P_1, P_2)$ in the probability space for two sets of parameters $(C_{13}/C_{12}$ and $C_{23}/C_{12})$ marked in (a), which represent the direct and indirect phases, respectively. The geodesics in each case are shown as black lines.

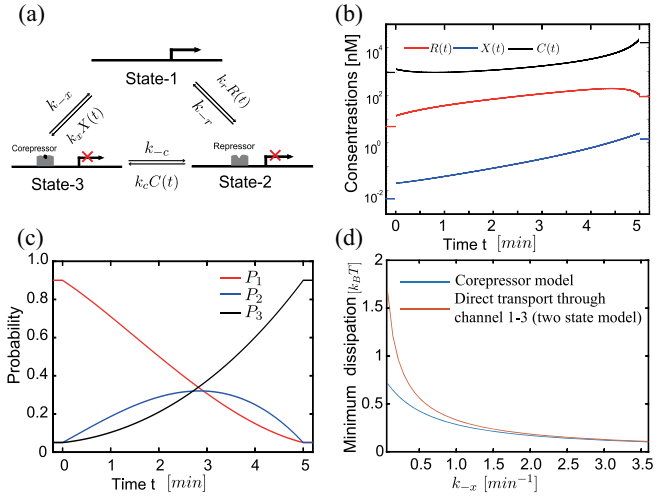

FIG. 3. (a) Biochemical network of a repressor-corepressor model, showing an operator site on DNA in three different states. Transition rate constants are given by [18] $k_{-r} = 1.68\ \text{min}^{-1}, k_{-c} = 0.72\ \text{min}^{-1}, k_{-x} = 0.072\ \text{min}^{-1}$ and $k_r = 0.0191\text{nM}^{-1}\,\text{min}^{-1}$, $k_c = 7.83 \times 10^{-4}\text{nM}^{-1}\,\text{min}^{-1}$, $k_x = 0.9\text{nM}^{-1}\,\text{min}^{-1}$. (b) The optimal protocol $X(t)$, $R(t)$, $C(t)$. (c) The optimal $\mathbf{P}(t)$ trajectory. (d) The difference of total entropy production between the original corepressor model and the direct transport model.

Discussion—In this Letter, we used a two-step approach to solve the OC problem in CRNs. In the adiabatic limit, a "Kirchhoff's law" applies, allowing us to show that the total dissipation is determined by a L_2 distance (the dissipation length) in the probability space with a dissipation metric that depends on probability and network topology. The optimal probability trajectory and the OC protocol can be obtained by solving the geodesic equation for minimizing this "dissipation length." Application of our theoretical approach to simple CRNs clearly demonstrates the importance of indirect paths in minimizing the energy cost of changing probability distribution and reveals a rich set of OC protocols depending on details of the network topology and capacity of each reaction. Our approach also leads to a tighter lower bound for the total dissipation that depends on the network topology in the adiabatic limit.

In most cellular biochemical networks, the pseudoreaction rate constants can be modulated by concentrations of proteins (e.g., enzymes) whose production can be controlled by transcription and translation of target genes, which are slower processes. For example, accumulation of the protein product can take many minutes to hours both in bacteria and eukaryotes (slower) [50,51]. However, the controlled system typically operate much faster than transcription [52], such as the enzyme catalysis (∼1–100 μ sec) [53,54], signal transduction (∼1 msec) [55,56], and even the regulation of the gene itself (transcription factor binding to DNA ∼ 1 sec) [57]. Thus, the adiabatic approximation ($\tau \gg \tau_R$) should be valid in most biochemical networks. Furthermore, our direct numerical results [58] with different values of τ for the fully connected three-node network (Fig. 1) show that the main conclusions and qualitatively features of the OC protocol and the corresponding optimal transport trajectory found in the adiabatic limit hold true for finite τ even down to the shortest control time τ_c, which is comparable to τ_R (see Sec. III.B in SM for details).

The notion of thermodynamic length established ∼40 years ago [32–34] has become an important concept in the study of stochastic thermodynamics recently. However, most previous studies focused on the thermodynamic length defined in the Riemannian manifold spanned by (mostly macroscopic) control parameters (e.g., the conjugate forces in the Hamiltonian) [22,23,35–38,61], whereas the "dissipation length" was derived directly in the probability (state) space in our Letter.

The connection between OC and optimal transport has been established in systems with continuous state variables governed by Langevin equations where the minimum dissipation is determined by a Wasserstein distance with Euclidean metric in the state space [28–31,43]. However, previous attempts in discrete systems have only led to a distance measure that also depends on the control parameters [transition rates $k_{ij}(t)$] [40,44]. Here, by using the Kirchhoff's law, we first determined the optimal rates as a function of probability. A true distance metric tensor $\mathbf{\Lambda}^*(\mathbf{P}, \mathbf{C})$ in the probability (state) space is then derived, which transforms the OC problem in the rate space into an optimal transport problem in the state space.

Our general approach can be applied to study more realistic problems with modifications. In addition to the thermodynamic cost considered in this Letter, we can include cost of control itself, which can depend on the rates as well as the rates of changing the rates. The number of controllable reactions can also be limited to a small subset of all reactions. An interesting question there is which are the key subset of reactions to control in order to achieve the desired change in probability distribution with minimum cost. Furthermore, the objective function can be extended beyond minimizing entropy production. Other functional costs (or benefits) such as the control time τ, accuracy, and robustness of the control process can also be included in the overall target function.

Finally, we note that the circuit analogy was first proposed to study steady-state behaviors of networks in a pioneering work by Schnakenberg [62]. However, as far as we know the Kirchhoff laws have not been applied in the context of OC. It would be interesting to investigate how to use other key concepts developed in [62] such as the cycle flux for studying optimal control of CRNs.

Acknowledgments—Y. T. acknowledges useful discussions with Mark Squillante, David Hathcock, and Qiwei Yu. The work by Y. T. is partially supported by a NIH Grant No. (R35GM137134). The work by Y. Z. and Q. O. is supported by the National Natural Science Foundation of China (Grant No. 12090054) and the Starry Night Science Fund of Zhejiang University Shanghai Institute for Advanced Study. Y. T. would like to thank the Center for Computational Biology at the Flatiron Institute for hospitality while a portion of this work was carried out.

[1] K. Sekimoto, *Stochastic Energetics*, 1st ed. (Springer, Berlin, Heidelberg, 2012).
[2] U. Seifert, Stochastic thermodynamics, fluctuation theorems and molecular machines, Rep. Prog. Phys. **75**, 126001 (2012).
[3] J. J. Hopfield, Kinetic proofreading: A new mechanism for reducing errors in biosynthetic processes requiring high specificity, Proc. Natl. Acad. Sci. U.S.A. **71**, 4135 (1974).
[4] T. L. Hill, *Free Energy Transduction and Biochemical Cycle Kinetics*, 1st ed. (Springer, New York, 2012).
[5] T. Schmiedl and U. Seifert, Stochastic thermodynamics of chemical reaction networks, J. Chem. Phys. **126**, 044101 (2007).
[6] R. Rao and M. Esposito, Nonequilibrium thermodynamics of chemical reaction networks: Wisdom from stochastic thermodynamics, Phys. Rev. X **6**, 041064 (2016).
[7] H. Qian, Phosphorylation energy hypothesis: Open chemical systems and their biological functions, Annu. Rev. Phys. Chem. **58**, 113 (2007).

[8] Y. Cao, H. Wang, Q. Ouyang, and Y. Tu, The free-energy cost of accurate biochemical oscillations, Nat. Phys. **11**, 772 (2015).
[9] G. Lan, P. Sartori, S. Neumann, V. Sourjik, and Y. Tu, The energy-speed-accuracy trade-off in sensory adaptation, Nat. Phys. **8**, 422 (2012).
[10] D. Zhang, Y. Cao, Q. Ouyang, and Y. Tu, The energy cost and optimal design for synchronization of coupled molecular oscillators, Nat. Phys. **16**, 95 (2020).
[11] A. C. Barato and U. Seifert, Thermodynamic uncertainty relation for biomolecular processes, Phys. Rev. Lett. **114**, 158101 (2015).
[12] A. C. Barato and U. Seifert, Cost and precision of Brownian clocks, Phys. Rev. X **6**, 041053 (2016).
[13] P. Pietzonka and U. Seifert, Universal trade-off between power, efficiency, and constancy in steady-state heat engines, Phys. Rev. Lett. **120**, 190602 (2018).
[14] J. Rodenfels, K. M. Neugebauer, and J. Howard, Heat oscillations driven by the embryonic cell cycle reveal the energetic costs of signaling, Dev. Cell **48**, 646 (2019).
[15] D. Del Vecchio, A. J. Dy, and Y. Qian, Control theory meets synthetic biology, J. R. Soc. Interface **13**, 20160380 (2016).
[16] J. A. Sharp, K. Burrage, and M. J. Simpson, Implementation and acceleration of optimal control for systems biology, J. R. Soc. Interface **18**, 20210241 (2021).
[17] P. J. Thomas, M. Olufsen, R. Sepulchre, P. A. Iglesias, A. Ijspeert, and M. Srinivasan, Control theory in biology and medicine, Biol. Cybern. **113**, 1 (2019).
[18] E. Ilker, O. Gungor, B. Kuznets-Speck, J. Chiel, S. Deffner, and M. Hinczewski, Shortcuts in stochastic systems and control of biophysical processes, Phys. Rev. X **12**, 021048 (2022).
[19] T. Schmiedl and U. Seifert, Optimal finite-time processes in stochastic thermodynamics, Phys. Rev. Lett. **98**, 108301 (2007).
[20] T. Schmiedl and U. Seifert, Efficiency at maximum power: An analytically solvable model for stochastic heat engines, Europhys. Lett. **81**, 20003 (2007).
[21] K. Proesmans, J. Ehrich, and J. Bechhoefer, Finite-time landauer principle, Phys. Rev. Lett. **125**, 100602 (2020).
[22] G. M. Rotskoff and G. E. Crooks, Optimal control in nonequilibrium systems: Dynamic riemannian geometry of the Ising model, Phys. Rev. E **92**, 060102 (2015).
[23] G. M. Rotskoff, G. E. Crooks, and E. Vanden-Eijnden, Geometric approach to optimal nonequilibrium control: Minimizing dissipation in nanomagnetic spin systems, Phys. Rev. E **95**, 012148 (2017).
[24] S. Blaber, M. D. Louwerse, and D. A. Sivak, Steps minimize dissipation in rapidly driven stochastic systems, Phys. Rev. E **104**, L022101 (2021).
[25] B. Remlein and U. Seifert, Optimality of nonconservative driving for finite-time processes with discrete states, Phys. Rev. E **103**, L050105 (2021).
[26] S. Blaber and D. A. Sivak, Optimal control with a strong harmonic trap, Phys. Rev. E **106**, L022103 (2022).
[27] S. Blaber and D. A. Sivak, Optimal control in stochastic thermodynamics, J. Phys. Comm. **7**, 033001 (2023).
[28] E. Aurell, C. Mejía-Monasterio, and P. Muratore-Ginanneschi, Optimal protocols and optimal transport in stochastic thermodynamics, Phys. Rev. Lett. **106**, 250601 (2011).
[29] M. Nakazato and S. Ito, Geometrical aspects of entropy production in stochastic thermodynamics based on wasserstein distance, Phys. Rev. Res. **3**, 043093 (2021).
[30] S. Ito, Geometric thermodynamics for the Fokker–Planck equation: Stochastic thermodynamic links between information geometry and optimal transport, Inf. Geom. **7**, 441 (2023).
[31] A. Dechant, S.-I. Sasa, and S. Ito, Geometric decomposition of entropy production in out-of-equilibrium systems, Phys. Rev. Res. **4**, L012034 (2022).
[32] F. Weinhold, Metric geometry of equilibrium thermodynamics, J. Chem. Phys. **63**, 2479 (1975).
[33] P. Salamon and R. S. Berry, Thermodynamic length and dissipated availability, Phys. Rev. Lett. **51**, 1127 (1983).
[34] B. Andresen, R. S. Berry, R. Gilmore, E. Ihrig, and P. Salamon, Thermodynamic geometry and the metrics of weinhold and gilmore, Phys. Rev. A **37**, 845 (1988).
[35] G. E. Crooks, Measuring thermodynamic length, Phys. Rev. Lett. **99**, 100602 (2007).
[36] D. A. Sivak and G. E. Crooks, Thermodynamic metrics and optimal paths, Phys. Rev. Lett. **108**, 190602 (2012).
[37] Y.-H. Ma, R.-X. Zhai, J. Chen, C. P. Sun, and H. Dong, Experimental test of the $1/\tau$-scaling entropy generation in finite-time thermodynamics, Phys. Rev. Lett. **125**, 210601 (2020).
[38] G. Li, J.-F. Chen, C. P. Sun, and H. Dong, Geodesic path for the minimal energy cost in shortcuts to isothermality, Phys. Rev. Lett. **128**, 230603 (2022).
[39] N. Shiraishi, K. Funo, and K. Saito, Speed limit for classical stochastic processes, Phys. Rev. Lett. **121**, 070601 (2018).
[40] T. Van Vu and Y. Hasegawa, Geometrical bounds of the irreversibility in markovian systems, Phys. Rev. Lett. **126**, 010601 (2021).
[41] K. Yoshimura and S. Ito, Thermodynamic uncertainty relation and thermodynamic speed limit in deterministic chemical reaction networks, Phys. Rev. Lett. **127**, 160601 (2021).
[42] A. Dechant, Minimum entropy production, detailed balance and wasserstein distance for continuous-time Markov processes, J. Phys. A **55**, 094001 (2022).
[43] T. Van Vu and K. Saito, Thermodynamic unification of optimal transport: Thermodynamic uncertainty relation, minimum dissipation, and thermodynamic speed limits, Phys. Rev. X **13**, 011013 (2023).
[44] K. Yoshimura, A. Kolchinsky, A. Dechant, and S. Ito, Housekeeping and excess entropy production for general nonlinear dynamics, Phys. Rev. Res. **5**, 013017 (2023).
[45] P. Muratore-Ginanneschi, C. Mejía-Monasterio, and L. Peliti, Heat release by controlled continuous-time Markov jump processes, J. Stat. Phys. **150**, 181 (2013).
[46] H. Ge and H. Qian, Physical origins of entropy production, free energy dissipation, and their mathematical representations, Phys. Rev. E **81**, 051133 (2010).
[47] In the adiabatic limit, the control process is carried out near-equilibrium: $P_i k_{ij} \approx P_j k_{ji}(1 + \mathcal{O}(\tau_R/\tau))$. Together with

the constraint $k_{ij}+k_{ji}=C_{ij}$, we have $R_{ij}\approx(1/2C_{ij})[(1/P_i(t))+(1/P_j(t))]$ to the leading order in $\mathcal{O}(\tau_R/\tau)$.

[48] The inverse here is formal, since $\mathbf{\Gamma}(\mathbf{R})$ is a singular matrix due to $\sum_i J_i(t)=\sum_i \dot{P}_i(t)=0$, see Sec. I.A in SM for the definition of the inverse.

[49] R. Wald, *General Relativity* (University of Chicago Press, Chicago, 2010).

[50] S. Proshkin, A. R. Rahmouni, A. Mironov, and E. Nudler, Cooperation between translating ribosomes and RNA polymerase in transcription elongation, Science **328**, 504 (2010).

[51] X. Darzacq, Y. Shav-Tal, V. De Turris, Y. Brody, S. M. Shenoy, R. D. Phair, and R. H. Singer, In vivo dynamics of RNA polymerase II transcription, Nat. Struct. Mol. Biol. **14**, 796 (2007).

[52] U. Alon, *An Introduction to Systems Biology: Design Principles of Biological Circuits* (Chapman and Hall/CRC, London, 2019).

[53] M. Stroppolo, M. Falconi, A. Caccuri, and A. Desideri, Superefficient enzymes, Cell Mol. Life Sci. **58**, 1451 (2001).

[54] L. Michaelis and M. M. L. Menten, The kinetics of invertin action, FEBS Lett. **587**, 2712 (2013).

[55] U. S. Bhalla and R. Iyengar, Emergent properties of networks of biological signaling pathways, Science **283**, 381 (1999).

[56] D. Bray, Protein molecules as computational elements in living cells, Nature (London) **376**, 307 (1995).

[57] T. Kalisky, E. Dekel, and U. Alon, Cost benefit theory and optimal design of gene regulation functions, Phys. Biol. **4**, 229 (2007).

[58] See Supplemental Material at http://link.aps.org/supplemental/10.1103/PhysRevLett.134.018001, which includes Refs. [59,60], for additional information about the numerical methods.

[59] A. Rao, A survey of numerical methods for optimal control, Adv. Astronaut. Sci. **135** (2010), https://www.researchgate.net/publication/268042868_A_Survey_of_Numerical_Methods_for_Optimal_Control.

[60] Imperial college London optimal control software, http://www.ee.ic.ac.uk/ICLOCS/default.htm.

[61] Z. Wang and J. Ren, Thermodynamic geometry of nonequilibrium fluctuations in cyclically driven transport, Phys. Rev. Lett. **132**, 207101 (2024).

[62] J. Schnakenberg, Network theory of microscopic and macroscopic behavior of master equation systems, Rev. Mod. Phys. **48**, 571 (1976).